Journal of Population Therapeutics & Clinical Pharmacology

RESEARCH ARTICLE
DOI: 10.53555/jptcp.v31i7.6923

DEVELOPMENT AND EVALUATION OF PHYTOSOMES OF QUININE SULPHATE FOR THE TREATMENT OF MALARIA

Maryam Musa Kallah[1*], Manish Yadav[2], Mohit Mangla[3]

[1*,2,3]School of Medical and Allied Science, G D Goenka University, Gurgaon

***Corresponding Author**: Maryam Musa Kallah
[*]School of Medical and Allied Science, G D Goenka University, Gurgaon
Email: mkallah2@gmail.com

ABSTRACT
Phytosomes containing quinine sulfate were prepared using the anti-solvent precipitation method, with six formulations (F1-F6) developed by varying quinine to soya lecithin ratios. Among these, formulation F3 exhibited superior characteristics, achieving an entrapment efficiency of 75.77% at a ratio of 1:3. Dissolution testing revealed enhanced drug release rates compared to pure quinine, with formulation F3 demonstrating the highest release (95.5%) within 120 minutes. Analysis of release kinetics indicated a first-order release pattern (R = 0.9956) and a diffusion-controlled mechanism (Higuchi model, R = 0.984). Fourier-transform infrared spectra confirmed the successful incorporation of quinine into phytosomes (F3) without chemical interaction or degradation, retaining characteristic peaks. These findings highlight formulation F3 as a promising candidate for further pharmacological investigation and therapeutic applications in enhancing quinine's bioavailability.

INTRODUCTION
The term "Phyto" pertains to plants, whereas "some" relates to structures resembling cells [1]. Phytosomes, also known as herbosomes, are vesicular drug delivery systems that improve the absorption and availability of poorly soluble drugs [2]. Phytosomes consist of phospholipids and natural active phytochemicals, combined in their structures through a reaction involving phosphatidylcholine (or other hydrophilic polar head groups) and plant extracts in a solvent that lacks hydrogen ions [3]. These formulations show enhanced pharmacological and pharmacokinetic characteristics compared to standard preparations. The lipid-soluble phosphatidyl component encapsulates the hydrophilic phytoconstituent-choline complexes entirely. Phytosomes offer significant advantages such as high drug encapsulation and demonstrate improved stability due to chemical bonds formed between the polar head of the amphiphile molecule and the phytoconstituent [4], and exhibit enhanced bioavailability [5]. Additionally, increased absorption rates allow for lower dosages of active constituents to achieve biological effects, including for polar phytoconstituents [6]. Quinine, derived from an alkaline extract of cinchona bark found in Andean forests, was initially used as a treatment for malaria infections. Its historical recognition began with its administration to treat tropical fever in the Countess of Chinchon in Peru. Introduced to Europe during the 17th century as Jesuit's bark, its effectiveness varied depending on the nationality of physicians and the quality, notably the bitterness, of the bark [7]. Since the Siege of Belgrade in 1717, cinchona bark has been used to combat malaria among soldiers. In 1777, James Lind, a member of the British Royal Navy, proposed that ships stationed on the Guinea coast of West Africa should carry ample supplies of

powdered bark and wine. These provisions were intended to be distributed as necessary to individuals traveling by boat up rivers and onshore [8].

Quinine was the standard treatment for severe malaria for a prolonged period; however, it has been associated with treatment resistance and various adverse effects such as tinnitus, deafness, and hypoglycemia. Rapid intravenous administration can lead to toxic levels, potentially causing blindness and even death [9].

Malaria gets its name from the Italian term "mal'aria," which translates to "bad air," reflecting the historical association of the disease with marshy environments [10]. It is an endemic parasitic disease transmitted by vectors, caused by protozoan parasites of the genus Plasmodium, prevalent in tropical and subtropical regions globally [11]. Plasmodium comprises over 200 species that infect mammals, birds, and reptiles. Malaria parasites typically exhibit host specificity [12]. Plasmodium falciparum, Plasmodium vivax, Plasmodium malariae, Plasmodium ovale, and Plasmodium knowlesi are the five recognized species of the genus Plasmodium responsible for causing malaria in humans [13,14].

The parasites go through a complex life cycle in both vertebrate hosts and a mosquito vector, involving both sexual and asexual reproduction. This complexity poses challenges for the development of drugs and vaccines [15].

MATERIALS AND METHODS

Materials

For the development of phytosomes, quinine sulphate and soya lecithin were obtained from central drug house Pvt. Ltd, Vardaan house, Delhi, India. Acetone was obtained from Shri chemicals, Rajahmundry, Andra Pradesh, India and all were of analytical grade.

Methodology

Estimation of UV spectra of quinine sulphate

The UV spectra of pure drug was examined by UV spectrophotometer Shimadzu.

Stock solution was made Initially, 10 mg of quinine was dissolved in 5 ml of acetone. The volume was then adjusted to 100 ml using phosphate buffer pH 6.8 to obtain a solution of 100 µg/ml.

From the stock solution, various dilutions were prepared as follows: 1 ml of stock solution was diluted to 10 ml to achieve a concentration of 10 µg/ml, 2 ml to 10 ml for 20 µg/ml, 3 ml to 10 ml for 30 µg/ml, 4 ml to 10 ml for 40 µg/ml, and 5 ml to 10 ml for 50 µg/ml.

After preparing the samples, readings were taken using a UV-visible spectrophotometer. Blank readings were first obtained to correct the baseline. The absorption spectrum of quinine sulfate was determined using a concentration of 20 µg/ml, identifying a peak absorption wavelength at 332 nm. Subsequent sample readings were taken at this wavelength using the spectrophotometer [65].

Solubility studies

The solubility of quinine sulfate was evaluated in various solvents, with the drug dissolved in excess amount to ensure saturation. The vials containing the solvent and quinine sulfate mixture were sealed to prevent evaporation. The mixtures were agitated by shaking gently to aid dissolution. They were then allowed to stand at room temperature for a specified period to reach equilibrium. Visual monitoring was conducted for signs of dissolution, such as clarity or the absence of visible particles [66].

Melting point

The melting point of quinine sulphate is determined to be 220°c. This indicates the purity and identity of the quinine sulphate used in the experiment [67].

Preparation of quinine phytosomes

Phytosomes of quinine were prepared by anti-solvent precipitation method Different ratios of quinine and soya lecithin, namely, 1:1, 1:2, 1:3, 2:1, 2:3,3:1, were taken in the compositions, as shown in Table 1.1.

In a 100 mL round bottom flask, quinine and soy lecithin were placed, and 15mL acetone was added which was refluxed for 2 h. To obtain the complex as a precipitate, 15mL of n-hexane was added after the solution had been concentrated. The precipitate was collected and stored for 24 h in a desiccator. Through #100 mesh, the dried precipitate was sieved. Powdered complex was stored in ambered colored bottles [68].

Table 1.1 composition of phytosomes formulation

Formulation	Drug(mg)	Lipid(mg)	Solvent(ml)	Anti solvent(ml)
F1(1:1)	250	250	15	15
F2(1:2)	250	500	15	15
F3(1: 3)	250	750	15	15
F4(2:1)	500	250	15	15
F5(2: 3)	500	750	15	15
F6(3:1)	750	250	15	15

Evaluation of prepared phytosomes

Particle size analysis

The particle size analysis of the formulated preparation was conducted using a Malvern Zeta Sizer at 25°C, employing laser light scattering for measurement. This technique utilizes an argon laser-based method and is commonly employed for assessing particle size and distribution. Prior to the study, 100 mg of the phytosome was ground and mixed in 10 ml of distilled water [69].

Determination of drug content

The drug content of the phytosome was determined by suspending exactly 100 mg of the complex in 10 ml of acetone. After preparing suitable dilutions for absorbance measurement, UV Spectroscopy at 332 nm was used for estimation. The drug content was calculated based on the specific absorbance observed [70].

Entrapment efficiency

The entrapment efficiency of the phytosome was evaluated using a cooling centrifugation method at 15000 rpm for 15 minutes at 4°C. The ability of the phospholipid complex to entrap the drug was determined using UV spectroscopy [71]. The percentage entrapment efficiency (%EE) was calculated using the following formula:

$$\%EE = (amount\ of\ drug\ added - amount\ of\ drug\ unentraped) \div amount\ of\ drug\ added \times 100$$

FT-IR spectroscopy

The confirmation of the phytosome complex was validated using FT-IR spectroscopy, which involved analyzing the complex along with its individual components and physical mixtures across a range of frequencies. FT-IR spectroscopy proved to be a valuable tool in ensuring the stability and integrity of the phytosomal drug formulation, both in micro dispersion in water and after incorporation of the pure drug [72].

Transmission electron microscopy (TEM)

Transmission electron microscopy (TEM) was employed to visually inspect the morphology of both powdered terbinafine HCL phytosome and various selected terbinafine HCL-phospholipid complex formulations. The phytosome formulation was diluted with a 0.01% solution and shaken for 10 minutes. A drop of the phospholipid complex was then placed onto a carbon-coated copper grid, ensuring a thin coating. Subsequently, the PC film was air-dried before imaging under TEM [73].

In vitro release profiles

In vitro drug release studies were conducted for both pure quinine and quinine phytosomes using a USP type II dissolution apparatus. The dissolution was carried out in 900 mL of phosphate buffer pH 6.8 at a temperature of 37±0.5°C and a stirring speed of 100 rpm

Phytosomes equivalent to 5 mg of quinine were introduced into the medium. At specified time intervals (5, 10, 15, 30, 45, 60, 90, and 120 minutes) over a 2-hour period, 5 mL of dissolution fluid was withdrawn through a filter. Each time, an equal volume of fresh medium was replenished, and the withdrawn sample was appropriately diluted and analyzed using a UV-visible spectrophotometer (Shimadzu UV 1800) at 332 nm [74].

Drug release kinetics

In this study, the in vitro release of the formulation was analyzed through drug release kinetic studies. The data from the prepared formulation were fitted into various equations to determine the kinetics model and percentage release of the optimized phytosome formulation.

The kinetic models used included the Zero-order equation, First-order equation, Higuchi's model, and Korsmeyer-Peppas equation to assess the percent release of the drug.

RESULTS AND DISCUSSION

Pre-formulation study of drug

Organoleptic properties

Organoleptic properties of drug quinine found to be as per USP monograph. The organoleptic properties of quinine were found to the given below table 1.2

Table 1.2 organoleptic properties of quinine

s.no	Properties	Inferences
1	Colour	White
2	Oduor	Odorless
3	Appearance	Fully powder
4	Taste	Bitter

Melting point

Table 1.3 Melting point of quinine sulfate

Drug	**Observed melting point**	**Reference melting point**
Quinine	220°	225°

UV spectroscopy determination of absorption maxima in acetone

Absorption maxima was found to be 332nm as shown in Figure 2.1

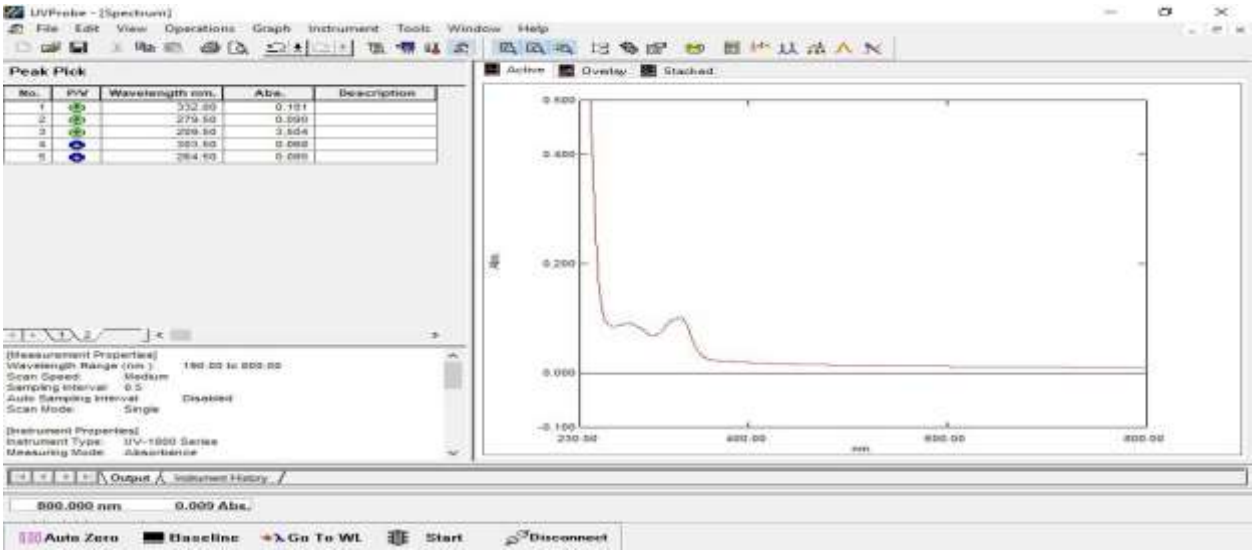

Figure 2.1 UV spectrum of quinine

Preparation of standard curve of quinine in acetone

The calibration curve of quinine was obtained and the absorbance was measured at 332nm.the calibration curve as shown in graph indicated the regression equation Y=0.0077 x +0.0318 and R^2 value 0.995, which shows good linearity.

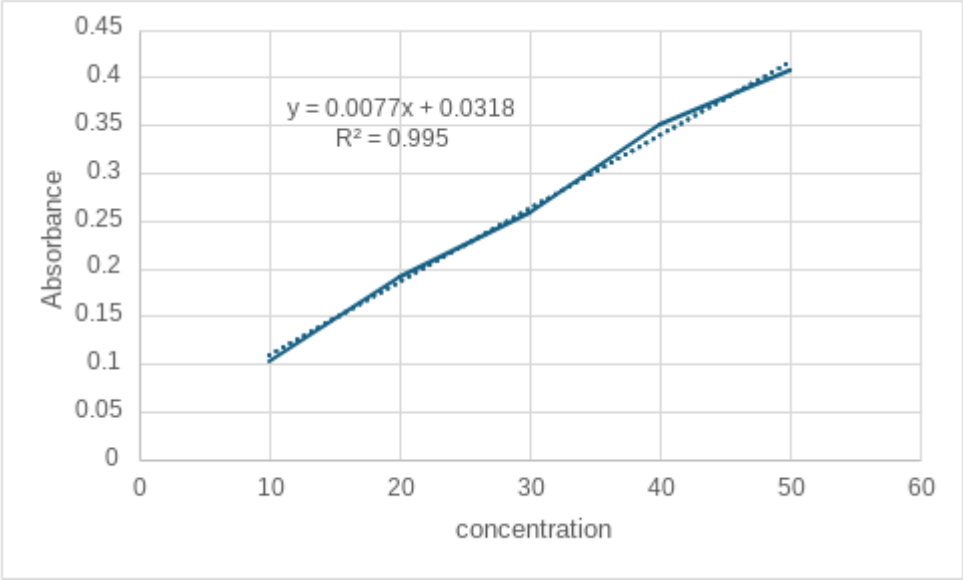

Figure 2.2 Graph of standard calibration curve of quinine in acetone

Solubility studies

Solubility of quinine is found to be determined with different solvents as shown in fig.2.5. Quinine was found to be highly soluble in acetone as well as DMSO 3mg/ml and 2mg/ml respectably and sparingly soluble in methanol and ethanol.

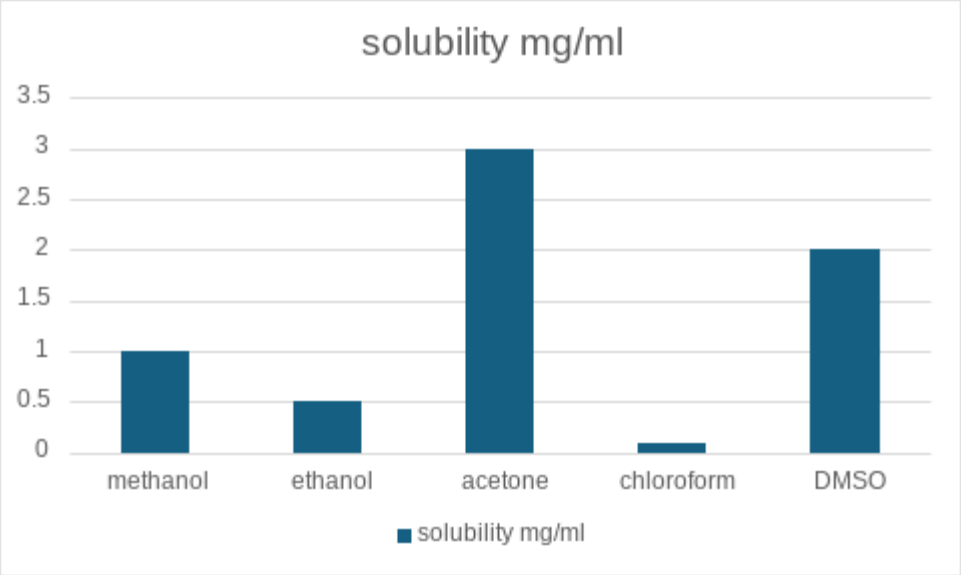

Figure 2.3 solubility of drug in different solvents

FT-IR Analysis

FT-IR was used to validate the establishment of the phytosomes of quinine sulfate as shown in fig2.4

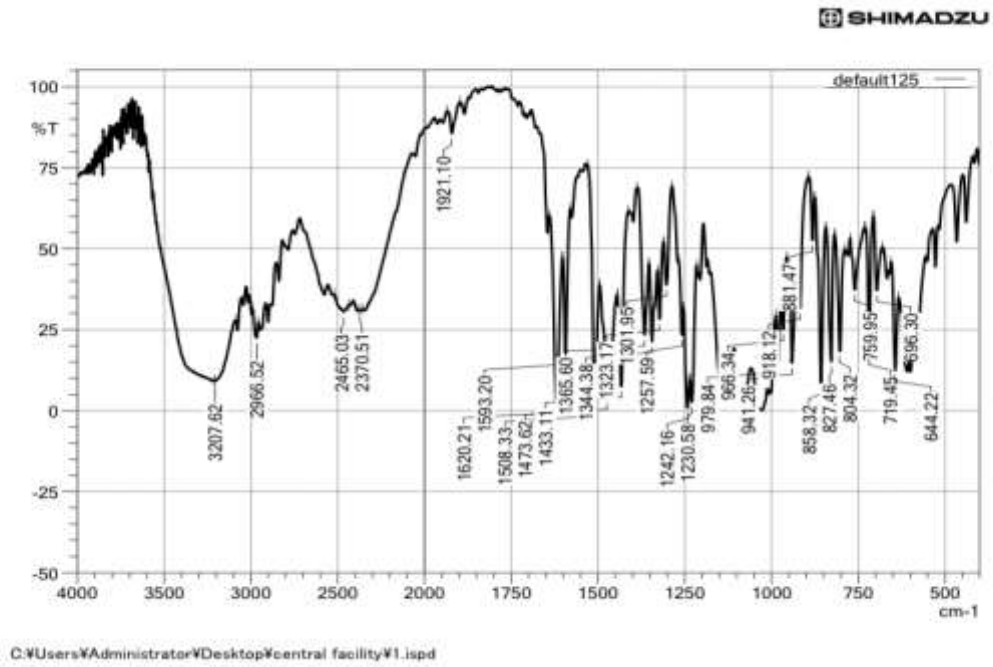

Figure 2.4 FT-IR spectra of pure quinine

Table 1.4 Interpretation of data from fig.2.4 (FT-IR spectra of pure quinine

S/no	FREQUENCY RANGE (cm^{-1})	FUNCTIONA GROUP	BOND TYPE
1	3207.62	Phenol	O-H stretching vibration
2	2966.52	Alkane	C-H stretching vibration
3	2465.09 and 2370.51	Nitrile	C≡N stretching vibration

4	1602.71 and 1593.20	Aromatic ring	C=C stretching vibration
5	1508.93	Amine	N-H bending vibration
6	1433.31	Alkane	CH_2 bending (scissoring) vibration
7	1365.60 and 1334.81	Alkane and Amine	CH_3 symmetric bending and C-N stretching
8	1242.16 and 1230.95	Amine	C-N stretching
9	1203.58	Ester	C-O stretching vibration
10	1157.30 and 1127.14	Ether	C-O stretching vibration
11	979.84 and 941.26	Aromatic	=C-H out of plane bending vibration
12	881.47	Aromatic	C-H out of plane bending
13	855.32	Aromatic	=C-H out of plane bending
14	822.46 and 804.32	Aromatic	C-H out of plane bending
15	759.95	Aromatic	C-H out of plane bending
16	719.45	Aromatic	C-H out of plane bending
17	644.22	Halogen compound	C-Cl stretching

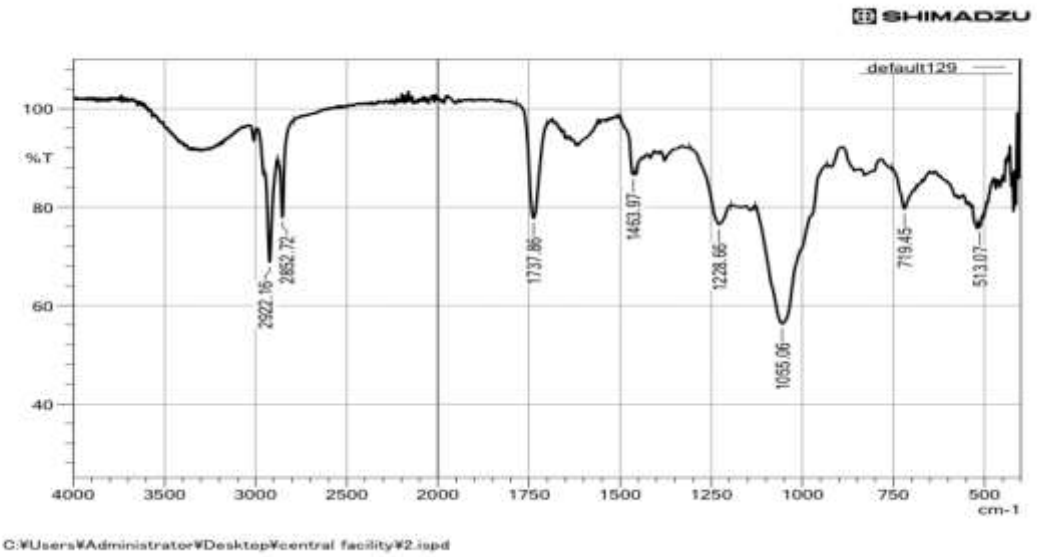

Figure 2.5 FT-IR spectra of Soya lecithin

Table 1.5 Interpretation of data from fig.2.5 (FT-IR spectra of soya lecithin).

S.no	FREQUENCY RANGE (cm^{-1})	FUNCTIONAL GROUP	BOND TYPE
1	2922.16 and 2852.72	Sp^3 C-H stretching	C-H stretching vibration
2	1737.86	Carbonyl	C=O stretching vibration
3	1463.97	Alkane	CH_2 and CH_3 bending vibration
4	1228.66	Ether	C-O stretching vibration
5	1055.06	Ester	C-O stretching vibration

6	719.45	Aromatic	C-H out of plane bending vibration
7	513.07	Halogen compound	C-Br stretching vibration

Evaluation of prepared phytosomes

Appearance of phytosomes

From the fiig.2.6 we observe a yellowish color appearance

Figure 2.6 Quinine – phospholipid complex phytosomes

Particle size analysis

The particle size with polydispersity index of formulation (F3) was 252 ± 101nm with PDI 0.151 in fig.2.7

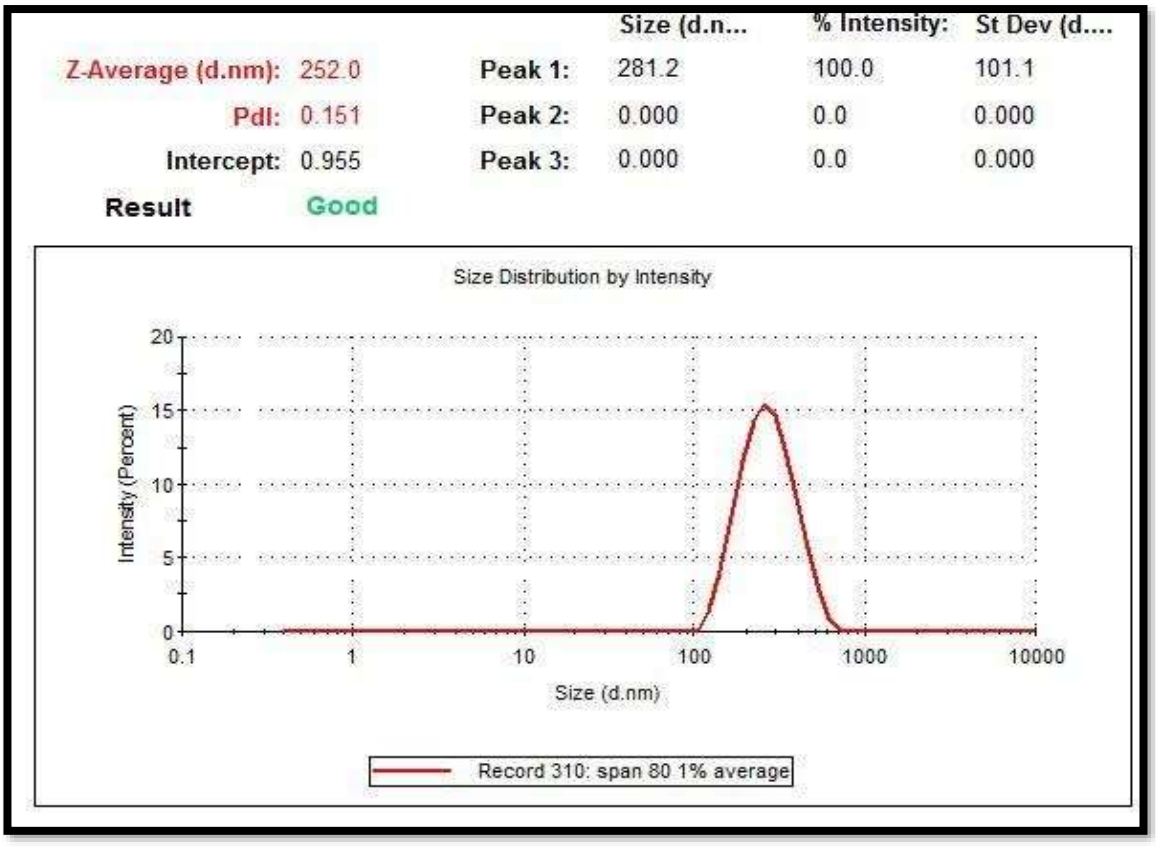

Figure 2.7 Particle Size Distribution of Phytosomes Formulation

Transmission electron microscopy (TTEM)

The image was established that the drug is completely encapsulated with the phytosome. The prepared formulation of quinine was exhibiting the effect results of physical entrapment of drug with the phospholipid molecules as shown in fig.2.8

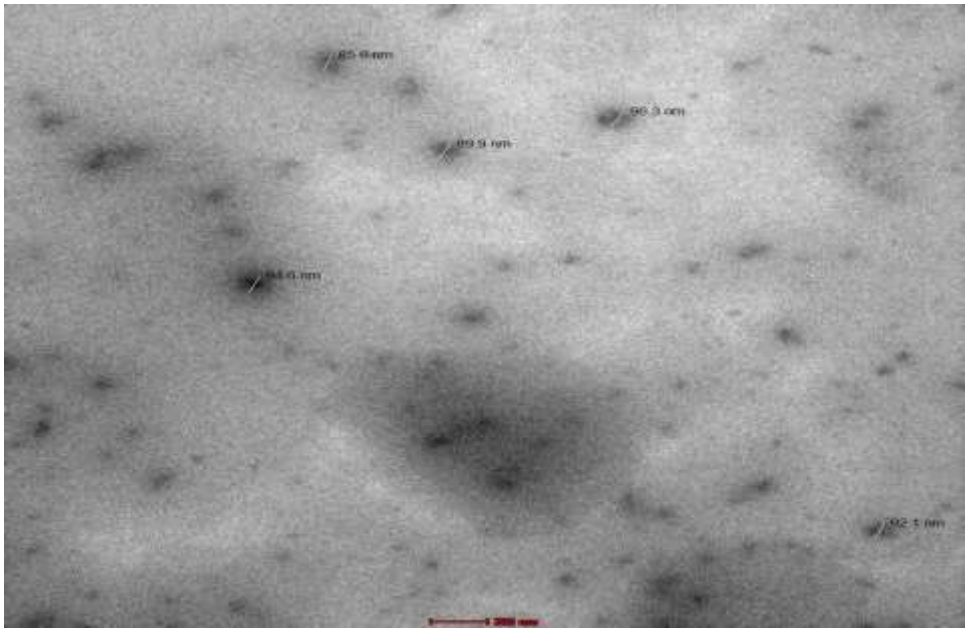

Figure 2.8 TEM image of selected formulation F3

FT-IR spectroscopy of phytosome formulation

Fourier-transform infrared spectra (FT-IR) of formulation of quinine sulfate phytosomes (F3) is shown in figure 2.11 and the interpretation of the data was given in table 3.6

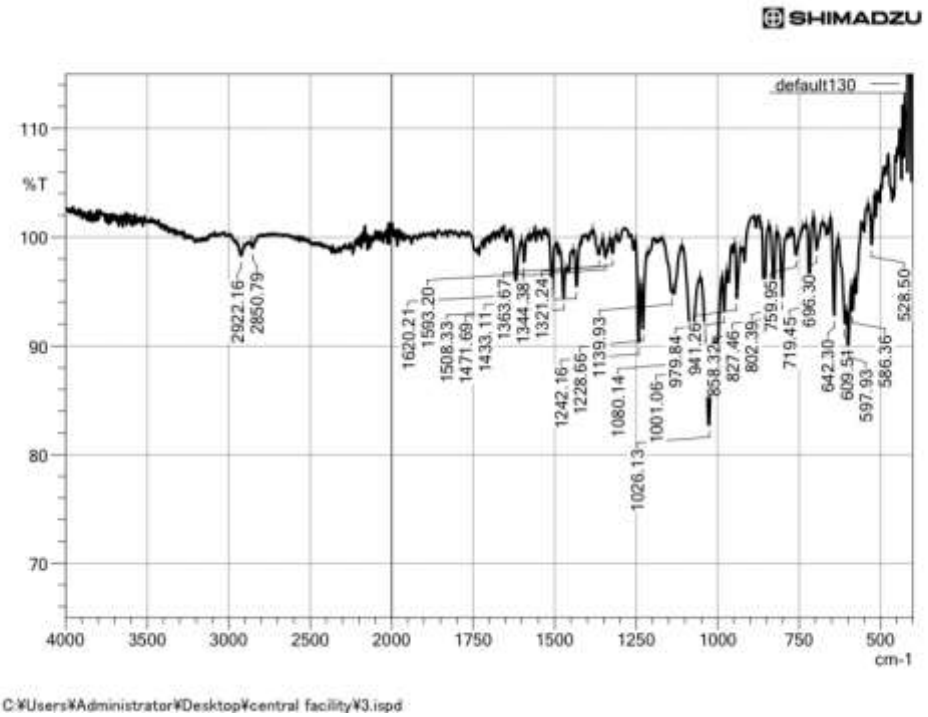

Figure 2.9 FT-IR of final formulation F3

Table 1.6 Interpretation of data from fig.2.9 (FT-IR spectra of formulation F3)

S.no	FREQUENCY RANGE (cm^{-1})	FUNCTIONAL GROUP	BOND TYPE
1	2922.16 and 2850.79	Alkane	C-H stretching vibration
2	1602.11	Aromatic ring	C=C stretching vibration
3	1508.93	Amine	N-H bending vibration
4	1471.63	Alkane	CH_2 bending (scissoring) vibration
5	1433.31	Alkane	CH_3 bending (asymmetric) vibration
6	1363.67 and 1321.24	Alkane and amine	CH_3 symmetric bending and C-N stretching
7	1242.16 and 1228.66	Amine	C-N stretching
8	1080.14 and 1039.93	Alcohol	C-O stretching
9	1026.13	Alcohol	C-O stretching
10	1001.06	Aromatic	Aromatic C-H in plane bending
11	979.84	Aromatic	=C-H out of plane bending
12	885.34	Aromatic	=C-H out of plane bending
13	820.43 and 719.45	Aromatic	C_H out of plane bending
14	642.30 and 596.30	Halogen compound	C-Cl stretching
15	586.65 and 582.50	Halogen compound	C-Br stretching

Drug Entrapment Efficiency

The drug entrapment efficiency values of the prepared phytosome of quinine (F1-F6) are shown in table 1.7.

Table 1.7 Entrapment Efficiency of Quinine Phytosomes

Formulation code	**% Entrapment Efficiency**
F1	72.71 ± 0.0011
F2	75.17±0.00090
F3	75.77±0.00085
F4	26.15±0.00092
F5	64.40±0.00088
F6	69.63±0.00093

In vitro drug release study

The invitro release studies of quinine from the phytosomes were studied in Phosphate buffer pH6.8. The results were are shown in table 1.8

Table 1.8 %Drug Delease of Quinine Phytosomes

Time (mins)	**pure drug**	**f1**	**f2**	**f3**	**f4**	**f5**	**f6**
0	0.00432±0.12 %	0.0036±0.15 %	0.0034±0.1 4%	0.00368±0. 13	0.00352±0. 16%	0.0038±0. 14%	0.00372± 0.15%
5	0.01359±0.21 %	0.0126±0.24 %	0.0117±0.2 3%	9.5±0.28	0.0122±0.2 6%	0.01309± 0.24%	0.01294± 0.25%
10	0.01449±0.25 %	0.0135±0.27 %	0.0127±0.2 6%	18.17±0.32	0.0133±0.2 8%	0.01419± 0.27%	0.01404± 0.28%

15	0.01449±0.25 %	0.0153±0.32 %	0.0144±0.3 1%	26±0.37	0.0153±0.3 4%	0.01638± 0.32%	0.02343± 0.39%
30	0.01449±0,25 %	0.01998±0.38 %	0.01872±0. 36%	38.5±0.42	0.02166±0. 40%	0.02367± 0.38%	0.02343± 0.39%
45	0.01449±0.25 %	0.02394±0.45 %	0.02196±0. 44%	52.8±0.48	0.02562±0. 46%	0.02763± 0.45%	0.02739± 0.46%
60	0.03141±0.49 %	0.02682±0.52 %	0.0243±0.5 1%	52.8±0.48	0.0288±0.5 3%	0.03114± 0.52%	0.03099± 0.53%
90	0.04041±0.55 %	0.03312±0.58 &	0.02952±0. 57%	85.2±0.60	0.03672±0. 59%	0.03996± 0.58%	0.03969± 0.59%
120	0.04131±0.61 %	0.03456±0.63 %	0.03018±0. 62%	95.5±0.65 %	0.03888±0. 64%	0.04176± 0.63%	0.03969± 0.59%

Drug Release Kinetics

In vitro drug release kinetics data of formulation F3 was given below

Table 1.9 Drug Release Kinetics of Quinine Phytosomes

Time (mins)	**% cumulative drug release**	**Log % cumulative drug release**	**%drug remained**	**Log % drug remained**	**Log time**	√time
0	0.003	-2.434	99.99	1.9998	0.000	0.000
5	9.500	0.978	90.50	1.956	0.699	2.236
10	18.70	1.272	81.30	1.910	1.000	3.162
15	26.00	1.415	74.00	1.869	1.176	3.872
30	38.50	1.586	61.50	1.789	1.477	5,477
45	52.80	1.723	47.20	1.674	1.653	6.708
60	65.00	1.813	35.00	1.544	1.778	7.745
90	85.20	1.930	14.80	1.170	1.954	9.486
120	95.50	1.980	4.500	0.653	2.079	10.95

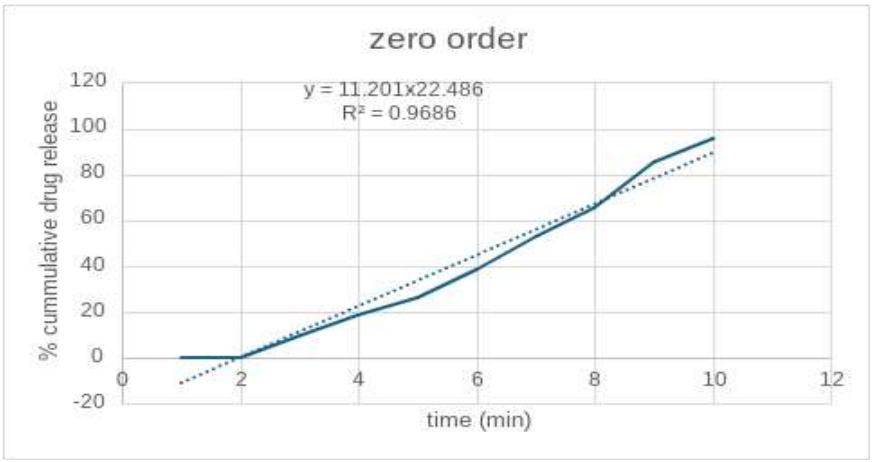

Figure 2.10 Zero order graph of formulation F3

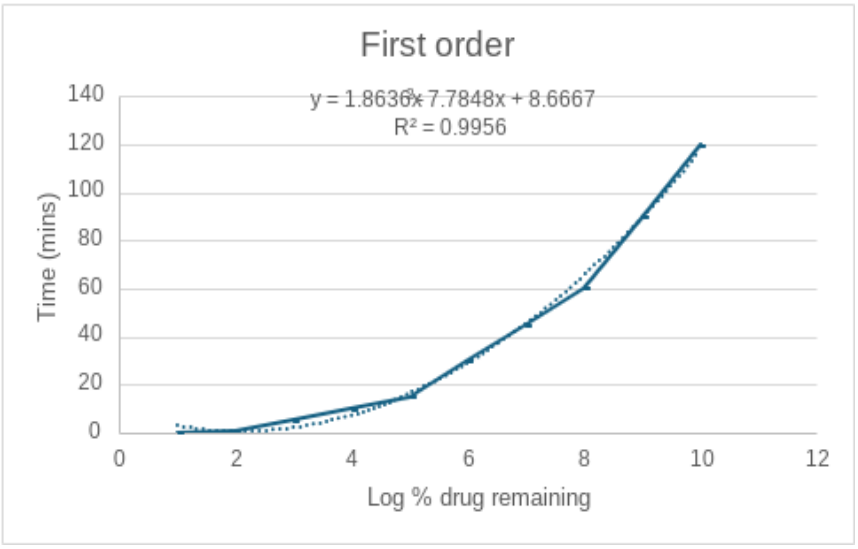

Figure 2.11 First order graph of formulation F3

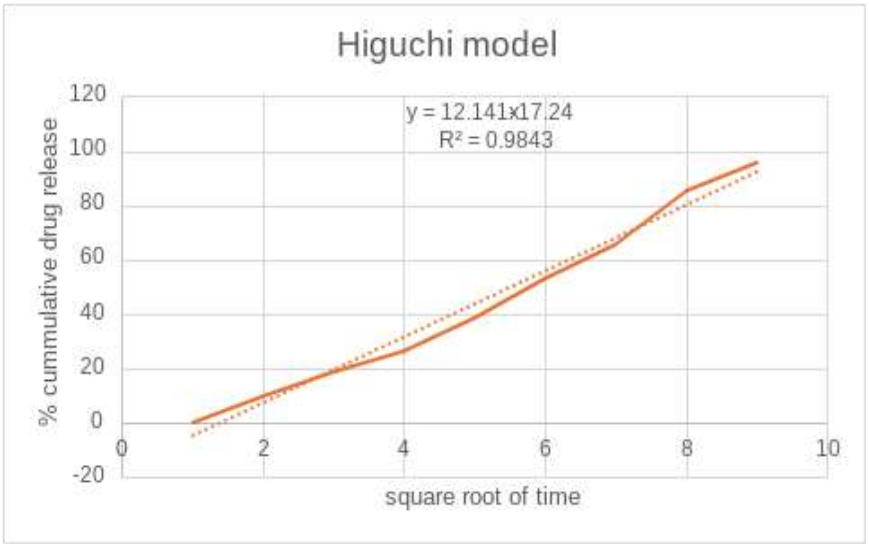

Figure 2.12 Higuchi order graph of formulation F3

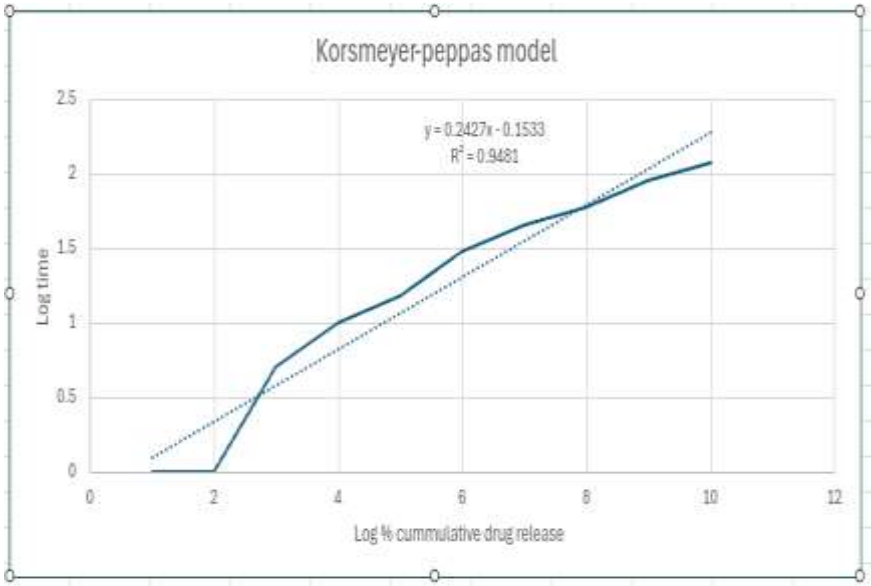

Figure 2.13 Korsmeyer Peppas Oder graph of formulation F3

Table 1.10 Correlation Coefficient, R^2 values

Plot	**R^2**
Zero order	0.968
First order	0.995
Higuchi	0.984
Korsmeyer's Peppas	0.948

DISCUSSION

Phytosomes containing quinine sulphate were successfully prepared using the anti-solvent precipitation method. Six formulations (F1-F6) were developed by varying the ratios of quinine to soya lecithin.

Among the formulations, F3 exhibited superior characteristics compared to others. The entrapment efficiency ranged from 26.15% to 75.77%, with the highest efficiency (75.77%) achieved in formulation F3, formulated with a quinine to soya lecithin ratio of 1:3. Dissolution testing was conducted on pure quinine and all six formulations. Enhanced drug dissolution rates were observed in the formulated phytosomes. Formulation F3 demonstrated the highest drug release (95.5%) within 120 minutes, prompting further investigation into its drug release kinetics.

Analysis of the release kinetics revealed that the drug follows first-order kinetics, supported by a high correlation coefficient (R = 0.9956), indicating a dose-dependent release pattern. The Higuchi plot (% cumulative drug release vs. square root of time) exhibited a linear relationship with a correlation coefficient of 0.984, suggesting diffusion as the predominant mechanism of drug release.

Fourier-transform infrared spectra (FTIR) of pure drug and promising formulation of phytosomes (F3) are shown. FTIR spectra of the drug showed its characteristic peak at 3207.62 cm^{-1} due to OH stretching, C=O stretching at 1921.10 cm^{-1}, aromatic ring C-C stretching at 1620.21 cm^{-1}, aromatic C-H bending at 1508.33 cm^{-1}, C-O stretching at 1242.16 cm^{-1}, and ortho-disubstituted aromatic C-H bending at 710.45 cm^{-1}. Phytosomes of formulation F3 revealed OH stretching at 2922.16 cm^{-1}, C=O stretching at 1620.21 cm^{-1}, aromatic ring C-C stretching at 1508.33 cm^{-1}, aromatic C-H bending at 1242.16 cm^{-1}, and ortho-disubstituted aromatic C-H bending at 710.45 cm^{-1}. The retention of characteristic peaks indicates successful incorporation of the drug into the phytosomes without significant chemical interaction or degradation.

CONCLUSION

The development of quinines ulphate -loaded phytosomes through the anti-solvent precipitation method proved successful, yielding six formulations (F1-F6) with varying quinine to soya lecithin ratios. Among these, formulation F3 demonstrated notable characteristics, including the highest entrapment efficiency of 75.77% at a ratio of 1:3 (quinine:soya lecithin). Dissolution studies indicated enhanced drug release rates compared to pure quinine, with formulation F3 exhibiting the most rapid release, reaching 95.5% within 120 minutes.

Further investigation into drug release kinetics revealed that quinine released from formulation F3 follows first-order kinetics, indicative of a predictable and dose-dependent release pattern. The Higuchi model analysis suggested that drug release predominantly occurs via diffusion.

FTIR spectroscopy confirmed the successful incorporation of quinine into phytosomes without significant chemical interaction or degradation, as evidenced by the retention of characteristic peaks observed in both the drug and formulation F3 spectra.

In conclusion, the formulation F3 of quinine-loaded phytosomes offers promising attributes for enhanced drug delivery, characterized by high entrapment efficiency, rapid and controlled drug release kinetics, and stability without adverse chemical alterations. These findings underscore the potential of phytosome technology in optimizing the therapeutic efficacy of quinine formulations.

REFERENCES

1. Nagar, G. (2019). Phytosomes: A novel drug delivery for herbal extracts. *Int J pharm sci Res*, *4*(3), 949-59.
2. Bhattacharya, S. (2009). Phytosomes: the new technology for enhancement of bioavailability of botanicals and nutraceuticals. *International journal of health research*, *2*(3), 225-232.
3. Kidd, P., & Head, K. (2005). A review of the bioavailability and clinical efficacy of milk thistle phytosome: a silybin-phosphatidylcholine complex (Siliphos). *Alternative medicine review*, *10*(3).
4. Dewan, N., Dasgupta, D., Pandit, S., & Ahmed, P. (2016). Review on-Herbosomes, A new arena for drug delivery. *Journal of pharmacognosy and phytochemistry*, *5*(4), 104-108.
5. Jain, N., Gupta, B. P., Thakur, N., Jain, R., Banweer, J., Jain, D. K., & Jain, S. (2010). Phytosome: a novel drug delivery system for herbal medicine. *Int J pharm sci drug Res*, *2*(4), 224-228.
6. Barani, M., Sangiovanni, E., Angarano, M., Rajizadeh, M. A., Mehrabani, M., Piazza, S., Gangadharappa, H. V., Pardakhty, A., Mehrbani, M., Dell'Agli, M., & Nematollahi, M. H. (2021). Phytosomes as Innovative delivery systems for phytochemicals: A comprehensive review of literature. *International journal of nanomedicine*, *16*, 6983–7022. https://doi.org/10.2147/IJN.S318416
7. Jovanović, A., & Krajnović, D. (2023). The developmental path of quinine: What can we learn from history? *Acta Medica Medianae*, *62*(2).
8. Fazal, T. M. (2024). *Military Medicine and the Hidden Costs of War*. Oxford University Press.
9. Garrido-Cardenas, J. A., González-Cerón, L., García-Maroto, F., Cebrián-Carmona, J., Manzano-Agugliaro, F., & Mesa-Valle, C. M. (2023). Analysis of fifty years of severe malaria worldwide research. *Pathogens*, *12*(3), 373.
10. Tuteja, R. (2007). Malaria− an overview. *The FEBS journal*, *274*(18), 4670-4679.
11. Escalante, A. A., & Pacheco, M. A. (2019). *Malaria molecular epidemiology: An evolutionary genetics perspective. Microbiol. Spectr. 7: 10.1 128/microbiolsec*. AME–0010–2019. doi: 10.1128/microbiolspec. AME-0010-2019.
12. Singh, B., & Daneshvar, C. (2013). Human infections and detection of Plasmodium knowlesi. *Clinical microbiology reviews*, *26*(2), 165-184.
13. Antony, H. A., & Parija, S. C. (2016). Antimalarial drug resistance: an overview. *Tropical parasitology*, *6*(1), 30-41.
14. White, N. J. (2008). Plasmodium knowlesi: the fifth human malaria parasite. *Clinical infectious diseases*, *46*(2), 172-173.
15. Guttery, D. S., Holder, A. A., & Tewari, R. (2012). Sexual development in Plasmodium: lessons from functional analyses. *PLoS pathogens*, *8*(1), e1002404.
16. Kanakapura, B., & Penmatsa, V. K. (2016). Analytical methods for determination of terbinafine hydrochloride in pharmaceuticals and biological materials. *Journal of pharmaceutical analysis*, 6(3), 137-149.
17. Katore, G. S., Bidkar, S. J., & Dama, G. Y. (2017). Formulation and evaluation of ciprofloxacin solid dispersion-controlled release floating capsules for solubility improvement. *Indian journal of pharmaceutical and biological research*, 5(03), 07-16.
18. Smith, E., Barkan, S., Ross, B., Maienthal, M., & Levine, J. (1973). Examination of quinidine and quinine sulphate and their pharmaceutical preparations. *Journal of pharmaceutical sciences*, 62(7), 1151-1155.
19. Mund, A. K., Abhinasa, C., Singh, R. P., Kishore, K., Pangi, B. P., & Pasayat, M. K. (2019). Preparation and characterization of phytosome of Norbixin. *World journal of pharmacy and pharmaceutical sciences*, 8, 1045-1057.
20. Pandey, S., Goyani, M., Devmurari, V., & Fakir, J. (2009). Transferosomes: A novel approach for transdermal drug delivery. *Der Pharmacia Lettre*, 1(2), 143-150.
21. Ittadwar, P. A., & Puranik, P. K. (2017). Novel umbelliferone phytosomes: Development and optimization using experimental design approach and evaluation of photo-protective and antioxidant activity. *International journal of pharmacy and pharmaceutical sciences*, 9, 218-228.

22. Jeevana, J. B., & Ragalatha, M. P. (2019). Development and in vitro evaluation of phytosomes of naringin. *Asian Journal of pharmaceutical and vlinical research*, 12, 252-256.
23. Varde, N. M., Mehta, N. K., Thakor, N. M., Shah, V. A., & Upadhyay, U. M. (2012). Phytosomes: A potential phospholipid nanoparticulate carrier for the bioavailability enhancement of herbal extracts. *Pharmacie globale*, 3(10), 1.
24. Zhang, F., Koh, G. Y., Jeansonne, D. P., Hollingsworth, J., Russo, P. S., & Vicente, G. (2011). A novel solubility and maintenance of anticancer activity. *Journal of pharmaceutical sciences*, 100, 2778-2789.
25. Xie, J., Li, Y., Song, L., Pan, Z., Ye, S., & Hou, Z. (2017). Design of novel curcumin-soybean phosphatidylcholine complex-based targeted drug delivery system. *Drug delivery*, 24, 707-719.